Column Supported Embankments with Geosynthetic Encased Columns: Validity of the Unit Cell Concept

Majid Khabbazian[1]; **Victor N. Kaliakin**[2]; **Christopher L. Meehan**[3]

Abstract: Column supported embankments (CSEs) are used to overcome common problems associated with the construction of embankments over soft compressible soils. The use of granular columns as deep foundation elements for CSEs can be problematic in soft soils due to the lack of adequate lateral confining pressure, particularly in the upper portion of the column. Using a high-strength geosynthetic for granular column confinement forms geosynthetic encased columns (GECs); the confinement imposed by the geosynthetic increases the strength of the column, and also prevents its lateral displacement into the soft surrounding soil. This paper presents the results of finite element analyses of a hypothetical geosynthetic reinforced column supported embankment (GRCSE) (i.e., a CSE underlain by geosynthetic reinforcement) that is constructed with GECs as the deep foundation elements. Full three-dimensional (3-d), 3-d unit cell, and axisymmetric unit cell analyses of the GRCSE were carried out to investigate the validity of the unit cell concept. The effect of the degree of nodal constraint along the bottom boundary when numerically modeling GRCSEs was also studied in this paper. Numerical results show that a full 3-d idealization is required to more precisely determine the tension forces that are produced in the geosynthetic reinforcement that underlies the GRCSE. A number of design parameters such as the average vertical stresses carried by the GECs, lateral displacement of the GECs, and the maximum settlement of the soft foundation soil, however, can be successfully calculated using unit cell analyses.

DOI: 10.1007/s10706-014-9826-8

Keywords: Geosynthetics; Granular column; Geosynthetic encased column; Unit cell; 3-d finite element analysis.

Reference: Khabbazian, M., Kaliakin, V. N., and Meehan, C. L. (2015). "Column Supported Embankments with Geosynthetic Encased Columns: Validity of the Unit Cell Concept." *Geotechnical and Geological Engineering*, Springer, 33(3), 425-442. (doi:10.1007/s10706-014-9826-8)

Note: The manuscript for this paper was submitted for review and possible publication on March 27, 2014; approved for publication on October 8, 2014; and published online in January of 2015.

1 Introduction

When constructing embankments over soft compressible soils, it is usually necessary to use some form of ground improvement to overcome common geotechnical engineering problems in the foundation soil, such as bearing capacity failure, slope instability, lateral spreading, and large total and/or differential settlements. The use of column supported embankments (CSEs) offers numerous advantages over alternative ground improvement techniques in the realm of embankment construction, including: relatively rapid construction, comparatively small total and differential settlements, and protection of adjacent facilities (e.g., Collin 2004; Han et al. 2004).

When constructing CSEs, one or more layers of geosynthetic can be placed over the columns/pile caps to form a geosynthetic reinforced column supported embankment (GRCSE). The use of this type of geosynthetic "bridging layer" over the columns and soft soil foundation enhances the load transfer efficiency from the embankment to the deep foundation elements and reduces the required area replacement ratio of the columns (the area replacement ratio is defined as the ratio of the area of the column to the total area of the column plus its tributary area) (Lawson 1992; Russell and Pierpoint 1997; Kempton et al. 1998; Han and Gabr 2002). In addition to transferring embankment loads to the columns, the use of a geosynthetic re-

[1]Geotechnical Engineer, Earth Engineering Incorporated, East Norriton, PA 19401, U.S.A. (Formerly, Graduate Student, University of Delaware, Dept. of Civil and Environmental Engineering, 301 DuPont Hall, Newark, DE 19716, U.S.A.) E-mail: majid@udel.edu

[2]Professor, University of Delaware, Dept. of Civil and Environmental Engineering, 301 DuPont Hall, Newark, DE 19716, U.S.A. E-mail: kaliakin@udel.edu

[3]Bentley Systems Incorporated Chair of Civil Engineering & Associate Professor, University of Delaware, Dept. of Civil and Environmental Engineering, 301 DuPont Hall, Newark, DE 19716, U.S.A. E-mail: cmeehan@udel.edu (corresponding author)

inforcement layer also helps to resist horizontal thrust at the sides of an embankment, which eliminates the need for using inclined columns in this area.

In GRCSEs, the columns have the important role of transferring the surcharge and embankment loads from the ground surface to a stiffer underlying layer. A wide range of deep foundation systems (i.e., stiff or non-stiff columns) can be used in GRCSE construction. In very soft soils, however, it is well understood that the use of granular columns can be problematic due to the lack of adequate lateral confining pressure, particularly in the upper portion of the column. Using a high-strength geosynthetic for encasement of granular columns increases the strength of a given column and improves its stress-displacement response (e.g., Al-Joulani and Bauer 1995; Alexiew et al. 2005; Murugesan and Rajagopal 2007; Khabbazian et al. 2009, 2010a, b); the resulting foundation elements are commonly referred to as geosynthetic encased columns (GECs).

The field behavior of GRCSEs is truly three-dimensional (3-d), as each column is not continuous in the out-of-plane direction (e.g., Kempton et al. 1998; Liu et al. 2007; Huang et al. 2009; Jenck et al. 2009). The complicated mechanism of load transfer in GRCSEs combines arching effects, tension in the geosynthetic reinforcement, and stress concentrations (Han and Wayne 2000).

Smith and Filz (2007) performed axisymmetric and 3-d analyses of GRCSEs. In these analyses the columns were relatively stiff (e.g., deep-mixed soil-cement) and thus not encased. Square pile caps topped the columns. Smith and Filz (2007) stated that 3-d numerical analyses are necessary to calculate the strains and tensile forces that develop in orthotropic geosynthetic reinforcement. They also stated that stress concentrations in the geosynthetic reinforcement at the corner of a square pile cap can only be captured through a 3-d numerical analysis.

Some 3-d analyses of GRCSEs and CSEs have been performed to simulate the behavior of a row of columns in the transverse direction (e.g., Huang et al. 2006, 2009; Liu et al. 2007; Jenck et al. 2009; Wachman et al. 2010). Three-dimensional analyses have also been performed to capture the behavior of a "unit cell" (e.g., Kempton et al. 1998; Stewart and Filz 2005; Chew et al. 2006). The columns in these analyses were, however, not encased.

Even though 3-d analyses are most appropriate for the numerical simulation of GRCSEs and CSEs, the majority of past numerical models of these geostructures have assumed the solution domain to be two-dimensional (2-d). These analyses have historically been performed assuming either plane strain (e.g., Jones et al. 1990; Kempton et al. 1998; Han et al. 2005, 2007; Yan et al. 2006; Oh and Shin 2007; Tan et al. 2008; Huang et al. 2009; Zheng et al. 2009) or axisymmetric (e.g., Han and Gabr 2002; Vega-Meyer and Shao 2005; Smith and Filz 2007; Chen et al. 2008; Tan et al. 2008; Borges et al. 2009; Huang et al. 2009; Zheng et al. 2009; Plaut and Filz 2010) idealizations.

The concept of a "unit cell" has been the most popular approach for numerically simulating the response of CSEs when GECs are used as the deep foundation elements (e.g., Murugesan and Rajagopal 2006; Malarvizhi and Ilamparuthi 2007; Park et al. 2007; Almeida et al. 2013; Elsawy 2013). Yoo and Kim (2009) compared the results of axisymmetric, 3-d unit cell, and fully 3-d models of CSEs with GECs, but without geosynthetic reinforcement placed over the columns. They concluded that the results of 3-d unit cell analyses were in good agreement with those from a fully 3-d model; however, axisymmetric modeling tended to give results that were 10-20% larger than the 3-d models, particularly for the vertical effective stress and lateral deformation of the granular columns, as well as for the strain in the geosynthetic encasement.

A detailed review of available literature has thus revealed that no research has been performed to investigate the behavior of GRCSEs with GECs, either in a 2-d or 3-d idealization. Consequently, this paper presents the results of 2-d and 3-d finite element analyses that were carried out to study the validity of the unit cell concept in the numerical simulation of GRCSEs that utilize GECs as the deep foundation elements.

2 Finite Element Modeling

2.1 *Geometry, Boundary Conditions, and Loading*

A finite element analysis approach was selected for purposes of numerically simulating the behavior of the GRCSE and foundation soils. For purposes of analysis, a hypothetical embankment underlain by a geosynthetic layer and constructed over GECs was simulated. The cross-section of the idealized embankment, the soft soil, and the GECs are shown in Fig. 1a. Due to symmetry about the z-axis, only one-half of the solution domain was modeled in the full 3-d analyses. The height of the embankment was assumed to be 5 m, with a 1V:2H side slope. In all of the finite element analyses that were performed, the thickness of the soft soil and the length of the GECs were assumed to be 5 m. It was also assumed that the soil and GECs were underlain by a rigid layer. GECs with a diameter of 0.8 m and a center-to-center spacing of 1.6 m were selected for the numerical analyses. The resulting area replacement ratio (ARR) was thus 20%. This value was selected in accordance with observations made by Han et al. (2004), who reported that the ARR for GRCSEs typically ranges between 5 and 30%. As shown in Fig. 1a, a single layer of geosynthetic reinforcement over the GECs was assumed.

To investigate the soundness of the unit cell concept as it applies to the numerical modeling of GRCSEs, three configurations were analyzed: a full 3-d idealization (Fig. 1c), a 3-d unit cell idealization (Fig. 1d), and a 2-d axisymmetric unit cell idealization (Fig. 1e).

In the full 3-d analysis, only a single row of columns was considered, as these types of embankments are usually long and have a uniform cross-section in the transverse direction. Furthermore, because of symmetry in the longitudinal direction (about the z-axis), only half of a row of columns and the surrounding soft soil was modeled in the full 3-d analyses (Fig. 1c). In these analyses, the lateral ex-

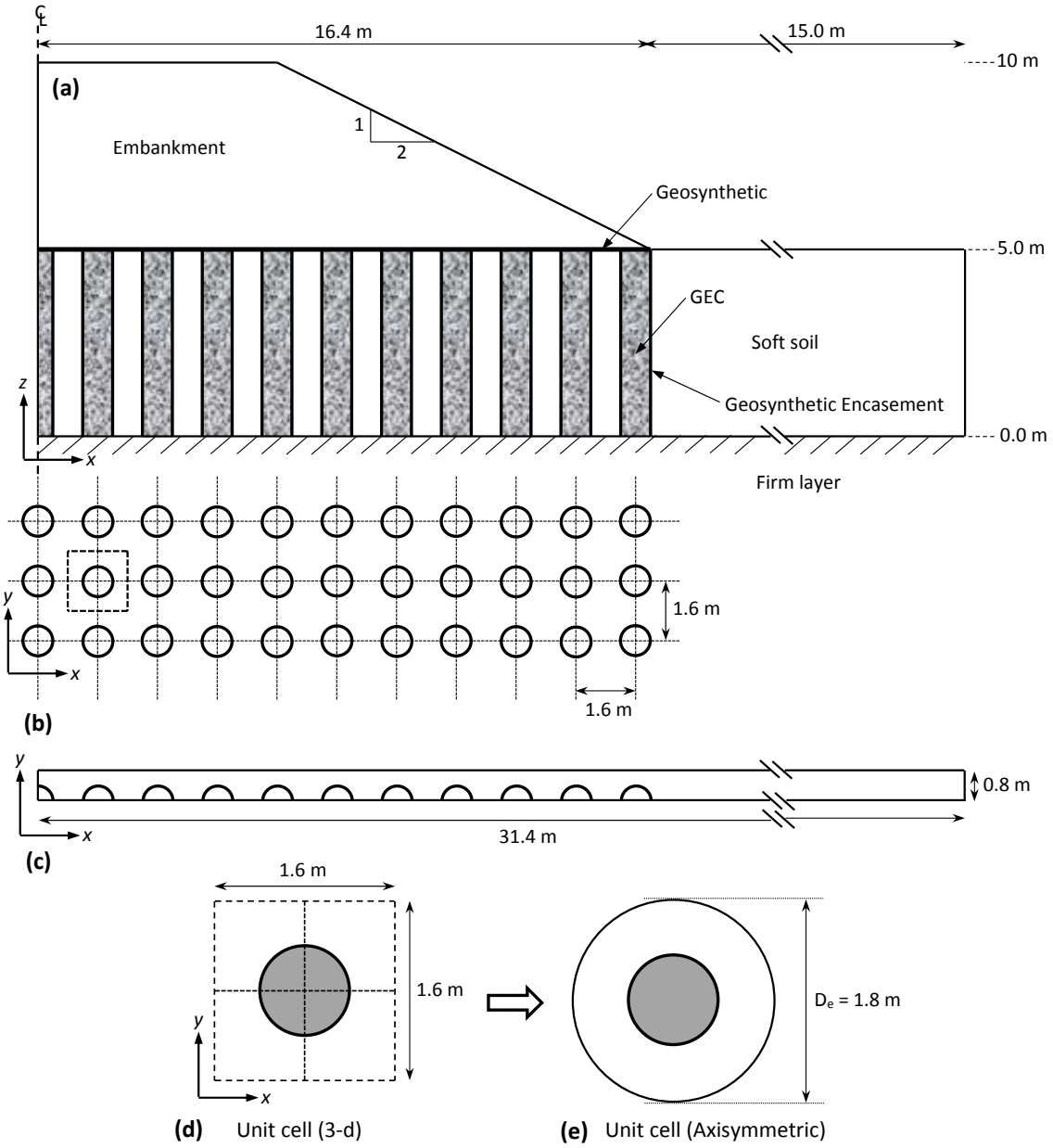

Fig. 1: (a) Cross section of the simulated GRCSE embankment, (b) plan view of GECs, (c) plan view of the full 3-d simulation, (d) plan view of a unit cell, and (e) plan view of an equivalent axisymmetric unit cell.

tent of the soft soil beyond the toe of the embankment was chosen to be 15 m. Sensitivity analyses were performed to confirm that the finite element results were not affected by the imposed conditions at this distance along the right vertical boundary of the soft soil.

A unit cell consists of a single column surrounded by the tributary area of soil that is defined by lines of symmetry (Fig. 1b). For columns in a square configuration with equal center-to-center spacing in both the longitudinal and transverse directions, the unit cell has a square geometry (Fig. 1d). A 3-d finite element analysis is required to properly model this unit cell. Since it has two lines of symmetry (Fig. 1d), only one-quarter of the unit cell was modeled in the finite element analyses.

As shown in Fig. 1e, a square unit cell can be approximated by a circular one by choosing the same area of soft soil that surrounds the column. The resulting circular unit cell can be used to perform axisymmetric finite element analyses. In this case, the equivalent diameter of the unit cell is equal to 1.13 times the center-to-center column spacing; i.e., $D_e = (1.13)(1.6) = 1.80$ m.

It should be noted that for columns in a triangular pattern, the unit cell forms a regular hexagon around the column. This hexagonal unit cell can also be closely approximated by an equivalent circular unit cell with the same total area. The equivalent circular unit cell can then be simulated using either a 3-d unit cell or an axisymmetric unit cell. This approximation is similar to that

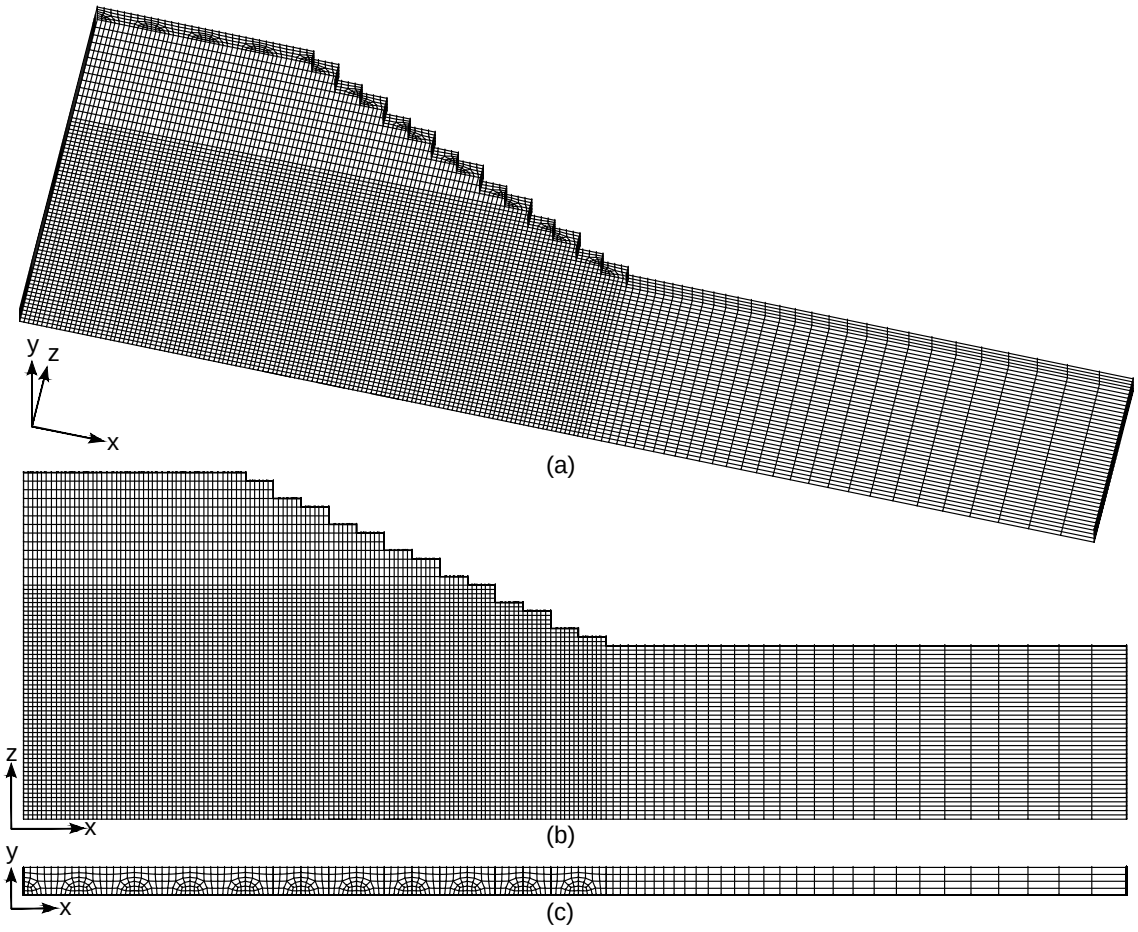

Fig. 2: Finite-element mesh used for full 3-d analysis: (a) three-dimensional view, (b) profile view, and (c) plan view.

in which a square unit cell is approximated by a circular unit cell, as discussed in the previous paragraph. In other words, nearly identical analyses can be performed to numerically simulate the unit cell behavior of GRCSEs with either square or triangular column configurations; only the unit cell areas are slightly different. It is expected that the results from a full 3-d analysis of a triangular column spacing configuration would be also slightly different than that for a square column spacing, since the cross-section in the transverse direction in the case of the triangular pattern is not uniform. The differences in the numerical simulations of GRCSE with columns in triangular and square patterns are beyond the scope of this paper. For purposes of the analyses conducted herein, a square pattern spacing was exclusively assumed.

In the full 3-d model (Fig. 2), nodal displacements in the x-direction are constrained along the right and left boundaries (planes) of the solution domain. These boundary conditions are reasonable, because: (1) the left side planar boundary represents a symmetry boundary, which cannot have displacements that are normal to the plane (i.e., in the x-direction), and (2) the right side planar boundary is far enough away (e.g., the soft soil domain is large enough) that constraining the nodal displacements in the x-direction along this boundary has no significant effect on the model results. The boundary planes parallel to the x-z plane are also symmetry planes (recall Fig. 1c). It follows that nodal displacements in the y-direction (i.e., those normal to the x-z plane) must be constrained along these planes. Finally, along the bottom boundary, nodal displacements in the z-direction are constrained so as to prevent rigid-body motion in this direction.

In the 3-d unit cell model (Fig. 3), planes parallel to the x-z and y-z planes represent symmetry boundaries. As such, nodal displacements normal to these planes must be constrained. Along the bottom boundary, nodal displacements in the z-direction must be also constrained so as to prevent rigid-body motion in this direction.

In the axisymmetric unit cell model (Fig. 4), nodal displacements in the radial direction are constrained along the right and left boundaries of the solution domain. The latter specifications are necessitated by the fact that the left boundary represents a symmetry boundary, thus precluding displacements normal to it. Along the bottom boundary, nodal displacements in the z-direction are constrained so as to prevent rigid-body motion in this direction. The above nodal constraints associated with the full 3-d, 3-d unit cell, and axisymmetric unit cell analyses shall be referred to throughout the remainder of this paper as the "standard degree of nodal constraint" along the bottom

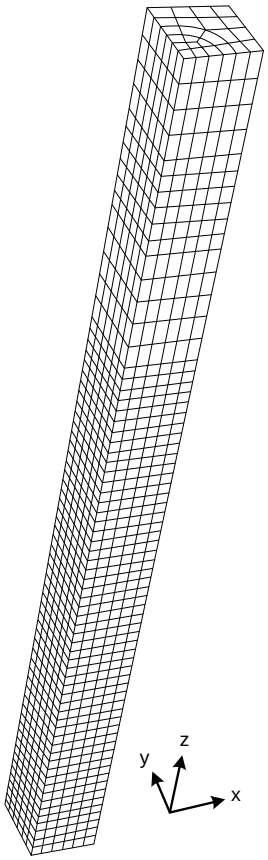

Fig. 3: Finite-element mesh used for 3-d unit cell analysis.

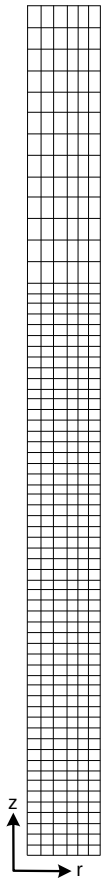

Fig. 4: Finite-element mesh used for axisymmetric unit cell analysis.

boundary of the solution domain.

Due to lateral spreading of the embankment in the full 3-d analysis, it was hypothesized that the numerical results might be affected by the imposed boundary conditions that are specified in the x-direction along the bottom of the solution domain (i.e., along the bottom of the soft soil and GECs). As a result, the full 3-d, 3-d unit cell, and axisymmetric unit cell analyses of the GRCSE were repeated with nodes along the bottom boundary constrained in all directions. These nodal constraints shall be referred to herein as the "increased degree of nodal constraint" along the bottom boundary of the solution domain. The results from analyses with both the "standard" and "increased" degrees of nodal constraint along the bottom boundary will be compared and discussed later in this paper.

All finite element analyses described herein were performed using the computer program ABAQUS (Hibbitt et al. 2007). The finite element analyses were initiated by activating the initial stresses in the GECs and in the surrounding soft soil. The initial lateral earth pressure was assumed to be at an 'at-rest' condition. The lateral earth pressure coefficient (K) was determined to be 0.5, using the empirical relationship proposed by Brooker and Ireland (1965), $K_o = 0.95 - \sin\phi$. After establishing the initial stress state, the embankment construction was simulated in a number of steps. The embankment loading was modeled by progressively assigning gravity to each 0.5 m thick layer of elements in the embankment. In all of the analyses the excess pore pressures were assumed to have dissipated over time, i.e., the analyses were considered to be "drained".

2.2 *Finite Element Mesh*

The finite-element mesh for the granular columns, the soft soil, and the embankment was developed using 8-node brick elements and 4-node quadrilateral elements in the 3-d and axisymmetric numerical simulations, respectively. The geosynthetic for both the column encasement and the reinforcement over the columns was modeled using 4-node quadrilateral and 2-node membrane elements in the 3-d and axisymmetric finite element analyses, respectively.

The finite-element meshes used for the full 3-d, 3-d unit cell, and the axisymmetric unit cell analyses are shown in Figs. 2, 3, and 4, respectively. For the full 3-d analysis, 38,856 continuum and membrane elements were used in the mathematical model, while only 1,840 and 448 elements were used in the finite-element mesh for the 3-d unit cell and the axisymmetric analyses, respectively. Mesh sensitivity analyses were performed to ensure that the meshes were sufficiently fine so as to yield accurate results. In order to minimize possible errors due to the finite element mesh, the same size of elements were utilized in all numerical analyses. It should also be noted that to eliminate ill-shaped elements in the finite-element mesh that was used

for the full 3-d analysis, the embankment slope was idealized in steps rather than a continuous slope (Fig. 2). By examining the number of elements that was used in the finite-element meshes, it can be observed that the full 3-d analysis is computationally much more expensive than numerical modeling of the unit cell either under 3-d or axisymmetric conditions.

2.3 *Constitutive Models*

The granular materials were idealized using an isotropic linear elastic - perfectly plastic model with a Mohr-Coulomb failure criterion. The Mohr-Coulomb model is defined by five parameters, namely: the effective friction angle (ϕ), effective cohesion (c), dilation angle (ψ), elastic modulus (E), and Poisson's ratio (ν). For both the embankment and columns, the granular soil was assumed to be loose Sacramento River sand. The following Mohr-Coulomb model parameter values were used to characterize the granular materials: $\phi = 35.0°$, $c = 0.0$, $\psi = 0.0°$, $E =$ 30,000 kPa, and $\nu = 0.20$. Kaliakin et al. (2012) discuss the determination of these values from experimental data for loose Sacramento River sand from tests performed by Lee and Seed (1967).

The soft soil was assumed to be normally consolidated Bangkok clay (Balasubramanian and Chaudhry 1978), and was idealized using the modified Cam Clay model. Khabbazian et al. (2012) investigated the effect of the soft soil constitutive model when numerically modeling CSEs constructed with GECs as the deep foundation elements, and concluded that the use of the modified Cam Clay model is preferable over the Mohr-Coulomb or linear elastic models for accurately capturing the behavior of the soft soil between columns. Five parameters are associated with this model, namely the void ratio (e) at unit pressure, the slope of the critical state line (M), Poissons ratio (ν), and the slopes of the swelling and re-compression (κ) and virgin consolidation (λ) lines in void ratio - log p' space, where p' is the effective mean pressure. The specific model parameter values used to characterize the soil were determined by matching numerical model results with experimental data for soft Bangkok clay (Balasubramanian and Chaudhry 1978). This particular Bangkok clay classifies as a fat clay (CH), with index properties of $G_s = 2.72$, $LL = 118 \pm 2(\%)$, $PL = 43 \pm 2(\%)$, $PI = 75 \pm 4(\%)$. The following Cam clay model parameters were used to characterize the Bangkok clay: $\kappa = 0.09$, $\lambda = 0.51$, $M = 1.0$, $\nu = 0.3$, and $e = 2.0$ (at a unit pressure of 1 kPa).

The geosynthetic was assumed to be an isotropic linear elastic material with a Poisson's ratio of 0.3 (e.g., Murugesan and Rajagopal 2006; Liu et al. 2007) for both the column encasement and the embankment reinforcement. Alexiew et al. (2005) documented that design values of the encasement tensile modulus (J) between 2,000-4,000 kN/m were required for the geosynthetic used to encase granular columns on a number of different projects (J is also commonly referred to as the geosynthetic stiffness, e.g., Murugesan and Rajagopal 2006; Smith and Filz 2007). Consequently, a value of $J =$ 3,000 kN/m was used in the numerical simulation of the geosynthetic encasement. The thickness of the geosynthetic (t) was assumed to be 2 mm for all of the numerical analyses that were performed. Khabbazian et al. (2009) and Khabbazian (2011) indicated that using an isotropic linear elastic material that is capable of carrying both compressive and tensile stresses for encasement can increase the bearing capacity of GECs and adversely affect the shape of lateral displacement (bulging) of GECs. To properly account for the fact that the geosynthetic does not carry compressive loads, the "No Compression" option available in ABAQUS (Hibbitt et al. 2007) was adopted in the finite element analyses. This ensured that spurious compressive forces would not be predicted in the geosynthetic reinforcement. The tensile modulus of the embankment reinforcement was also assumed to be 3,000 kN/m.

The influence of using interface elements between the geosynthetic encasement and the surrounding granular and soft soils in the numerical simulation of individual GECs for single-element column loading has been studied by Khabbazian (2011); results of potential interest from that study have also been presented in a number of related publications (e.g., Khabbazian et al. 2010a, 2011a, b). However, as noted by Khabbazian (2011), there are a number of numerical issues associated with the use of interface elements between the geosynthetic and the surrounding soils when simulating the behavior of GECs in CSEs and GRCSEs using the ABAQUS computer program. As a result, in all of the finite element analyses that were performed herein, no interface elements were used between the geosynthetic and the surrounding soils; i.e., the membrane elements were fully tied to the solid elements. This assumption is consistent with the modeling approach that has been used by a variety of other researchers in this area (e.g., Murugesan and Rajagopal 2006; Lo et al. 2010; Yoo 2010).

3 Assessment of Results

Although many parameters can be used to assess the validity of the unit cell concept for the numerical simulation of GRCSEs with GECs, the following four quantities were selected for assessment purposes herein: the average vertical stress on top of the GECs, the maximum settlement of the soft foundation soil, the lateral displacement of the GECs, and the tension force in the geosynthetic reinforcement. In the full 3-d analysis, the first column located on the centerline of the embankment (Fig. 1c) was selected for purposes of comparison with the unit cell idealizations. This was done in order to minimize the "edge effects" in the full 3-d analysis; i.e., to account for the fact that columns closer to the edge of the embankment will behave differently than those near the middle, due to the increased lateral movement (lateral spreading) of the embankment near its edges. The validity of the unit cell concept, as applied to columns at different locations in a full 3-d analysis, is also examined in this paper.

3.1 *Numerical Simulations with Bottom Boundary Constrained Only in Vertical Direction*

Figure 5 shows the average vertical stresses carried by the GECs versus the height of the embankment for all analyses. From this figure it is apparent that all analyses give essentially the same value of vertical stress on top of the GEC. The maximum difference between the 3-d and axisymmetric analyses was approximately 15%, while those from the full 3-d and 3-d unit cell analyses differed by no more than 4%.

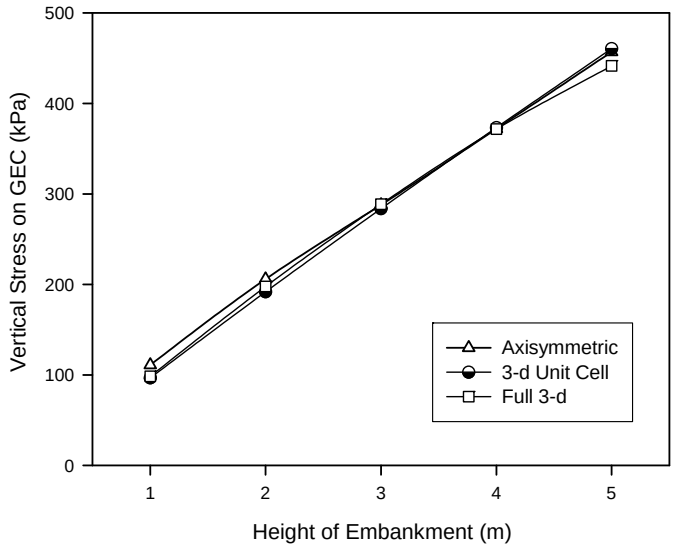

Fig. 5: Average vertical stresses on the GEC versus height of embankment for full 3-d, 3-d unit cell, and axisymmetric unit cell analyses ("standard" degree of nodal constraint along bottom boundary).

The second parameter studied in this section is the value of the maximum vertical displacement in the soft soil at the point farthest from the column (i.e., 1.13 and 0.9 m away from the center of the column for 3-d and axisymmetric analyses, respectively). Figure 6 presents the values of maximum vertical displacements for all the analyses. From this figure it is apparent that the results of the 3-d and axisymmetric unit cell analyses are in fairly good agreement; however, the maximum value of vertical displacement from the full 3-d analysis deviates somewhat from that obtained from the unit cell analyses. The difference between these results increases with the height of the embankment. For example, at an embankment height of 1 m the difference in the maximum vertical displacement calculated by the full 3-d and axisymmetric analyses equals 1.3 cm; however, this difference increases to 7.8 cm when the height of the embankment is increased to 5 m. The aforementioned differences are partly explained by the fact that, in the unit cell analyses, the extent of the solution domain in the direction parallel to the x-axis (Fig. 1) is dictated by the definition of the unit cell. No such restrictions are imposed in the full 3-d analysis. Consequently, less constraint is imposed on the soft soil in the 3-d analysis, which results in more lateral displacements and consequently larger vertical displacements as compared to the unit cell analyses.

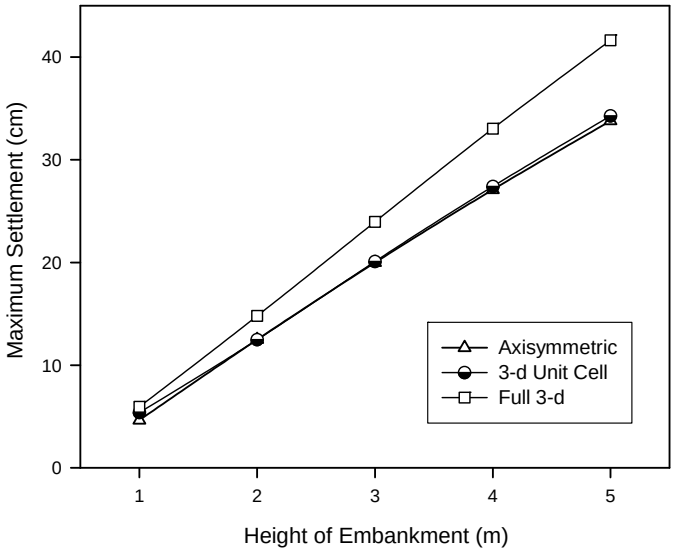

Fig. 6: Maximum settlement of foundation soft soil versus height of embankment for full 3-d, 3-d unit cell, and axisymmetric unit cell analyses ("standard" degree of nodal constraint along bottom boundary).

Figure 7 shows the lateral displacement (bulging) of the GECs for an embankment height of 5 m. From this figure it can be seen that, for most portions of the GEC, the lateral displacement values obtained from the full 3-d analysis are substantially greater than those from the unit cell analyses. The average calculated lateral displacement from the full 3-d analysis is significantly greater than that from the unit cell idealization. This is consistent with the explanation provided in conjunction with Fig. 6 concerning the extent of the solution domain in a direction parallel to the x-axis (Fig. 1).

It is clear from Fig. 7 that the values of lateral displacement for a GEC that result from finite element analysis do not vary smoothly with depth. The response that is shown is physically unlikely in light of the problem geometry, loading, and lateral constraint with depth. It is natural to suspect that such rather localized maxima may be the result of an overly coarse mesh. However, as noted in Sect. 2.2, sensitivity analyses were performed to ensure that the meshes used were sufficiently fine so as to yield accurate results. This somewhat oscillatory lateral displacement response that results from finite element analysis of GECs has also been reported by other researchers (e.g., Malarvizhi and Ilamparuthi 2007; Castro and Sagaseta 2009; Yoo and Kim 2009; Pulko et al. 2011). The precise reason for this lack of smoothness is not clearly known and the authors are currently studying this phenomenon.

Three columns, located different distances from the embankment centerline (measured in the x-direction, as shown in Fig. 1a-c), were selected from the full 3-d analy-

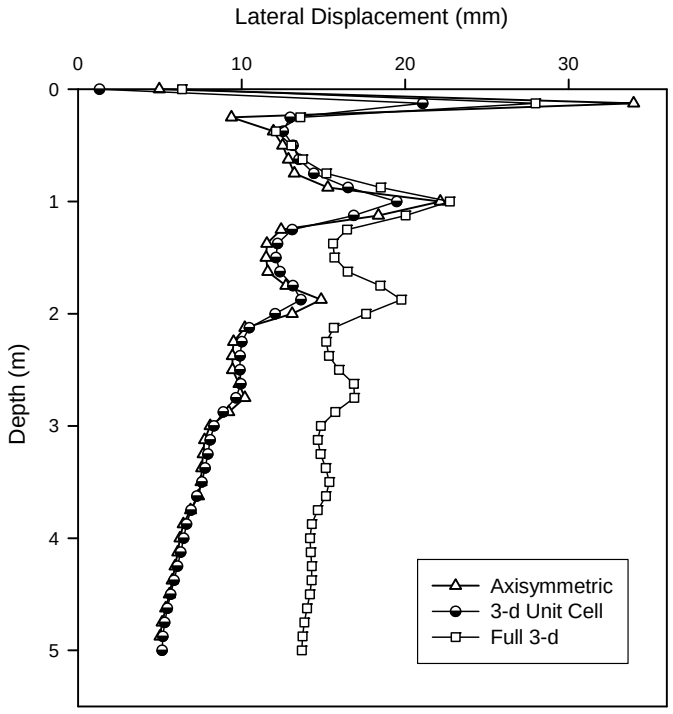

Fig. 7: Lateral displacement of the GEC versus depth for full 3-d, 3-d unit cell, and axisymmetric unit cell analyses at a height of embankment equal to 5 m ("standard" degree of nodal constraint along bottom boundary).

sis to investigate the sensitivity of the finite element results to the proximity of columns to the shoulder of the embankment. The first column was located on the centerline of the embankment; the second and the third columns were the third and fifth ones from the centerline of the embankment, respectively. The values of maximum vertical displacement of the foundation soil (i.e., settlement) around each of the columns as a function of the height of the embankment are shown in Fig. 8. For the sake of comparison, results from the 3-d and axisymmetric unit cell analyses are also shown in this figure. As evident from Fig. 8, the values of maximum settlements calculated in the 3-d analyses were almost the same for all three columns as long as the height of the embankment was less than 3 m. Once the height of the embankment exceeds 3 m, these values decrease with distance from the centerline of the embankment. For example, at an embankment height of 5 m, the value of the maximum settlement of the first column is about 20% greater than that for the fifth column. This is explained by the fact that the soft foundation soil closer to the embankment centerline is subjected to larger vertical stresses both at the ground surface and with depth as compared to the soil that is located closer to the shoulder. Such an effect is expected to be even greater if thicker layers of soft foundation soil were modeled in the numerical analyses. This observed model behavior represents another source of discrepancy between the values of vertical settlements calculated from unit cell idealizations and those from full 3-d models (Fig. 6). Similar trends as those shown for maximum settlement in Fig. 8 were generally observed for the other quantities such as the average vertical stresses carried by the GECs and the lateral displacement of the GECs. As a result, for the embankment analyzed herein, the design of the first GEC (i.e., the one located on the centerline of the embankment) is the most critical one.

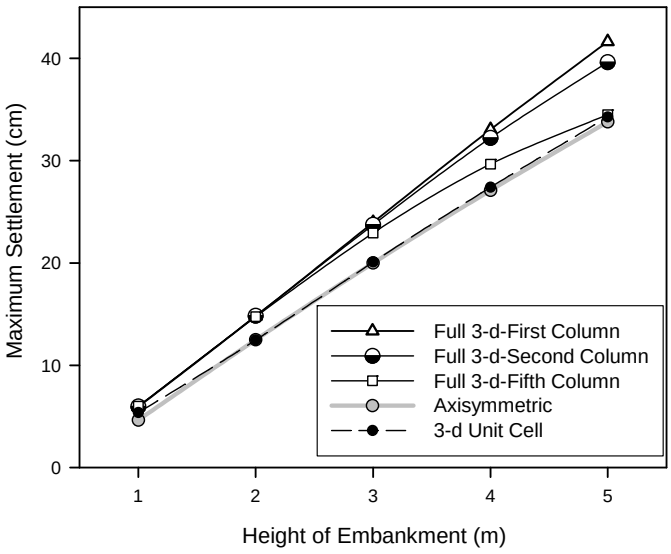

Fig. 8: Maximum settlement of soft foundation soil around GECs in a 3-d unit cell, axisymmetric unit cell, and full-3-d analysis versus the height of embankment, for GECs located at different distances from the embankment centerline ("standard" degree of nodal constraint along bottom boundary).

From the results shown in Figs. 5, 6, 7 and 8, for the most critical column in the embankment, it can be observed that the unit cell modeling approach (either the 3-d or axisymmetric) underestimates the maximum settlement between columns and the lateral displacement of GECs, but provides a reasonable estimate of the stresses applied to each column. As settlement is often the controlling factor in the design of GRCSEs, the use of a unit cell modeling approach can consequently lead to an unconservative design of such structures. It should be noted that this conclusion is based on results from analyses in which nodes along the bottom boundary of the soft soil and the GECs were unconstrained in the x and y-directions.

3.2 *Numerical Simulations with Increased Degree of Nodal Constraint along the Bottom Boundary*

Another set of finite element analyses, with full 3-d, 3-d unit cell, and axisymmetric unit cell idealizations, was carried out to study the soundness of the unit cell concept. The only difference between these analyses and those described in the previous section was that an "increased degree of nodal constraint" was imposed along the bottom boundary of the soft soil and the GECs, by also preventing displacement in the x-direction (see Fig. 1).

Figures 9, 10, and 11 present the average vertical

stresses on the GECs, the maximum settlement of the soft foundation soil, and the lateral displacement of the GECs for an embankment height of 5 m, respectively. Good agreement between all three analyses is evident in Figs. 9 and 11. As shown in Fig. 10, the greatest difference between the results of unit cell and full 3-d analyses was found to be in the prediction of maximum settlement of the soft foundation soil surrounding the GECs. For example, the difference between the maximum vertical displacement from the full 3-d and unit cell analyses was found to be 2 cm, which is significantly less than the 7.8 cm value that was obtained from analyses with a standard degree of nodal constraint along the bottom boundary.

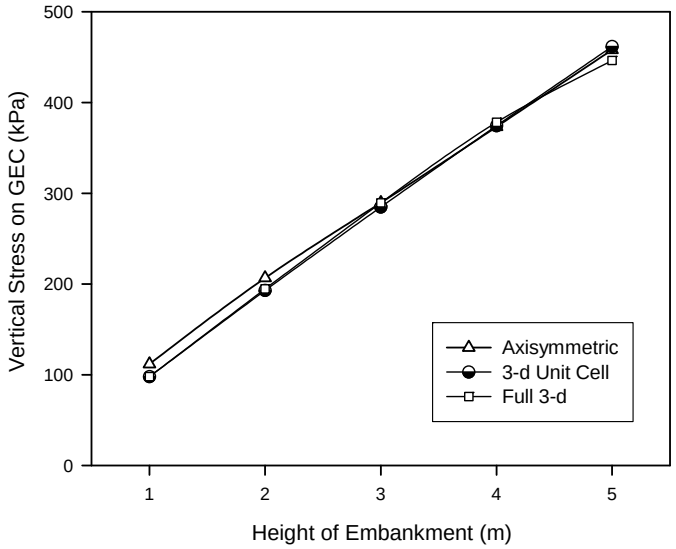

Fig. 9: Average vertical stresses on the GEC versus height of embankment for full 3-d, 3-d unit cell, and axisymmetric analyses (increased degree of nodal constraint along the bottom boundary).

Based on the results presented in Figs. 9, 10 and 11, it was confirmed that the numerical results for the 3-d and axisymmetric unit cell analyses were independent of the nodal constraints imposed along the bottom of the solution domain. This is not surprising since in both the unit cell idealizations all the loads are applied in the vertical direction. Due to the potential for lateral spreading of the embankment in the full 3-d analysis, the finite element results were affected by the nodal constraints imposed along the bottom of the soft soil foundation and GECs. In particular, the increased degree of nodal constraint along the bottom boundary in a full 3-d analysis gives results that are essentially the same as those from unit cell analyses. Thus, if the only quantities of interest are those shown in Figs. 9, 10 and 11, then unit cell analyses will provide quite accurate results with significantly lower computational effort as compared to full 3-d analyses.

Figure 12 shows the average stresses carried by three GECs in the full 3-d analysis (i.e., the first, third, and fifth column, as defined in the previous section) versus the

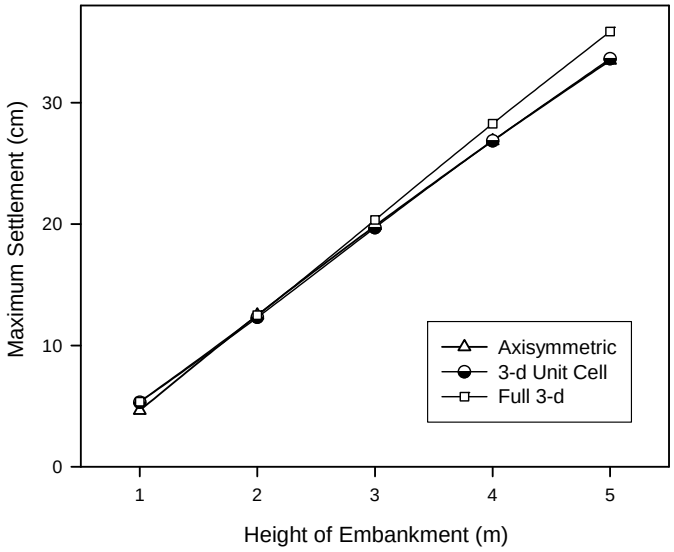

Fig. 10: Maximum settlement of foundation soft soil versus height of embankment for full 3-d, 3-d unit cell, and axisymmetric analyses (increased degree of nodal constraint along the bottom boundary).

height of embankment. The results of 3-d and axisymmetric unit cell analyses are also presented in this figure. As evident from Fig. 12, the stresses carried by the first and third columns are the same for the entire height of the embankment. However, for the fifth column, some minor deviations from the first and third columns can be seen after the height of embankment reaches 3 m. The difference between the vertical stresses carried by the first and fifth columns when the embankment height is 5 m is, however, only 12%. This is because there is less embankment load on top of the fifth column as compared to the first column. Further investigations showed similar trends for other parameters such as the vertical and lateral displacement of the GECs.

Further comparisons of the results of full 3-d analyses with standard and increased degree of nodal constraint at the bottom of the boundary of the soft soil and the GECs revealed that the average vertical stresses on the GECs were insensitive to the applied nodal constraints; however, the values of maximum settlement of the soft foundation soil and the lateral displacement of the GECs varied according to the fixity along the bottom boundary of the soft soil and the GECs.

3.3 *Tension Force in the Geosynthetic Reinforcement*

When designing GRCSEs, the tension force in the geosynthetic reinforcement due to vertical loads (i.e., the weight of embankment and any surcharge) in both the transverse and longitudinal directions is first calculated using the concept of a unit cell. There are currently a number of simplified methods that can be utilized for calculating this force (e.g., Carlson 1987; McKelvey 1994; BS8006 1995; Kempfert et al. 2004).

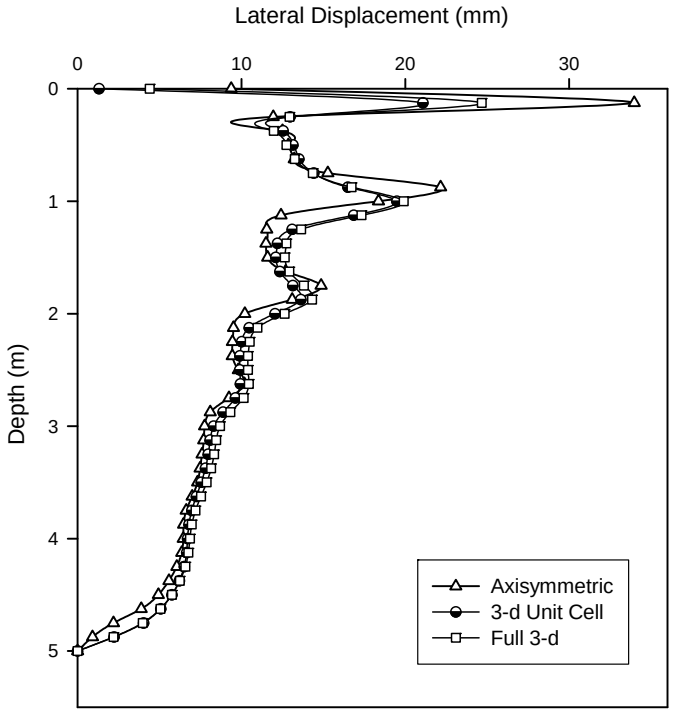

Fig. 11: Lateral displacement of the GEC versus depth for full 3-d, 3-d unit cell, and axisymmetric analyses at a height of embankment equal to 5 m (increased degree of nodal constraint along the bottom boundary).

In GRCSEs, the geosynthetic reinforcement layer also carries some additional forces that are induced by the embankment's tendency for lateral spreading. Consequently, the reinforcement must be designed to prevent, or at least minimize, lateral spreading of the embankment, while still performing its primary function of transferring vertical loads from the embankment to the top of the columns. The tension produced in the reinforcement (T) due to lateral spreading can be calculated by the following equation (Elias et al. 2006):

$$T = K_a(\gamma H + q)H/2 \tag{1}$$

where K_a is the coefficient of active earth pressure, which equals $\tan^2(45 - \phi/2)$, where ϕ is the effective friction angle of the embankment soil, γ is the unit weight of the embankment soil, q is the surcharge applied to the top of the embankment, and H is the height of the embankment. The tension force in the reinforcement due to the lateral spreading of the embankment is then added to the tension force in the transverse direction due to vertical loading.

The plan view of a 3-d unit cell located at the ground surface (i.e., where the horizontal geosynthetic reinforcement is placed) is shown in Fig. 13. Due to symmetry of the unit cell, the reinforcement tension forces in both directions shown in the highlighted regions are exactly the same. For an axisymmetric unit cell there is only one direction for the tension force in the geosynthetic reinforcement. Consequently the calculated reinforcement tension force in all directions is the same in analyses employing

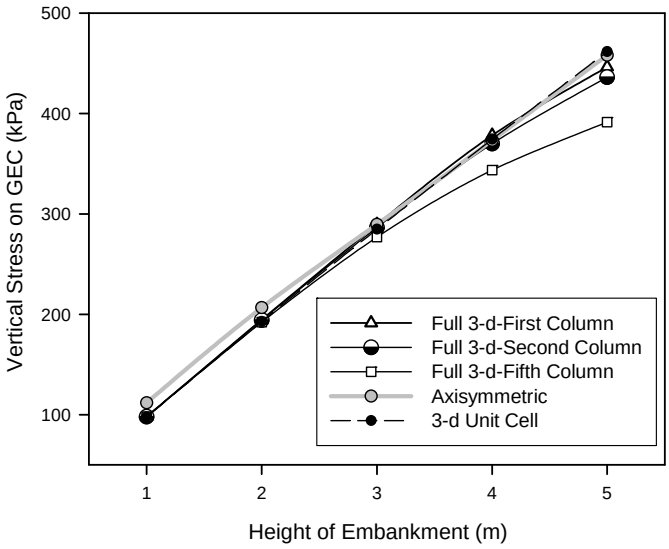

Fig. 12: Average vertical stresses on the GECs in a 3-d unit cell, axisymmetric unit cell, and GECs located at different distances from the embankment centerline in a full 3-d analysis versus the height of embankment (increased degree of nodal constraint along the bottom boundary).

an axisymmetric unit cell. In a full 3-d analysis, however, the tension force in the x-direction (Fig. 1) can be different than that in the y-direction due to the lateral spreading of the embankment in the transverse direction.

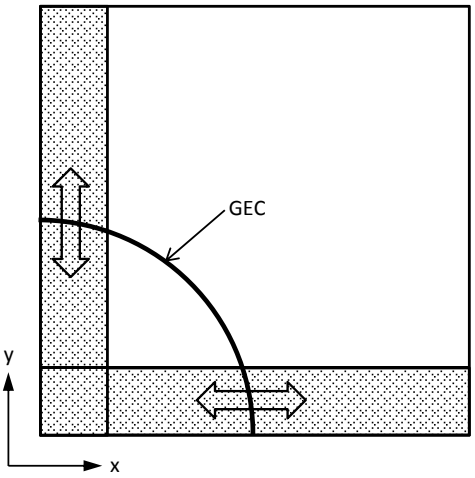

Fig. 13: Plan view of a 3-d unit cell.

As mentioned above, in existing design methods it is usually assumed that the tension force in the longitudinal direction of the embankment is less than that in the transverse direction, and is equal to the tension force calculated from the unit cell idealization. The validity of this assumption is now further investigated. This is done by first comparing the reinforcement forces in the transverse direction obtained from a full 3-d, a 3-d unit cell, and an axisymmetric unit cell analysis. Then the ability of the 3-d and axisymmetric unit cell idealizations for predict-

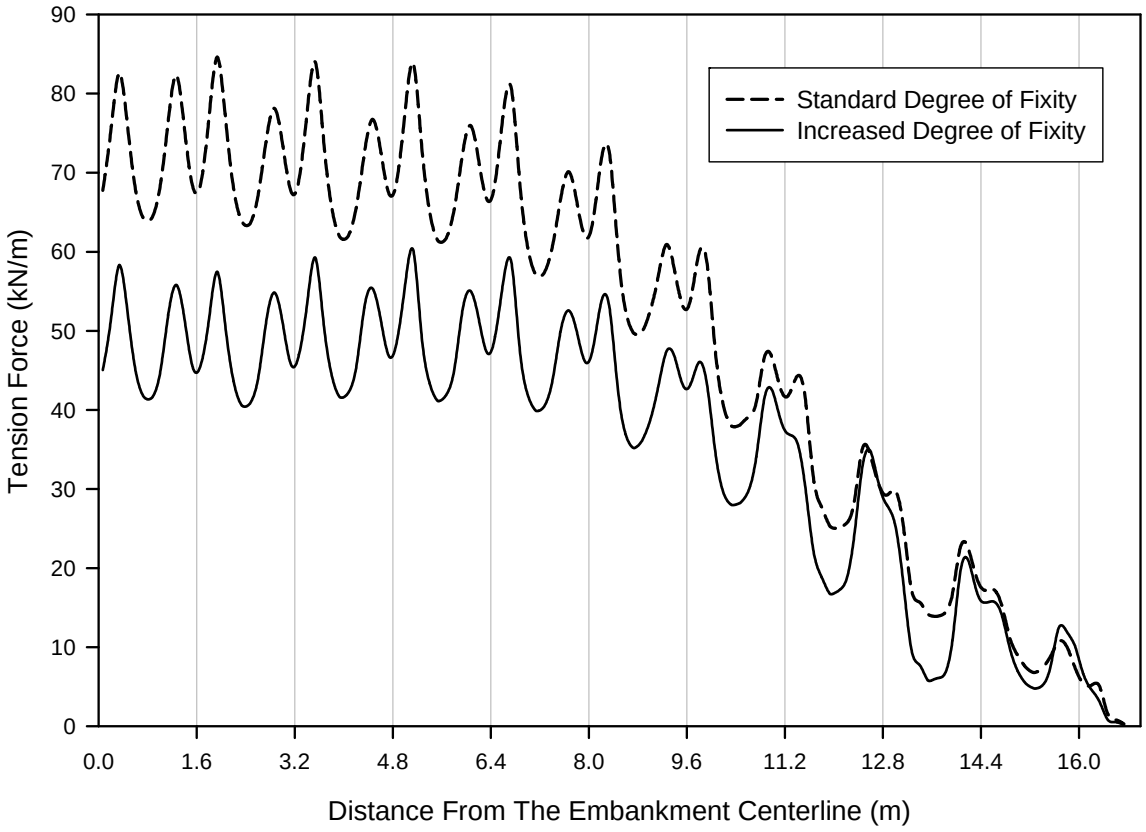

Fig. 14: Variation of tension force in geosynthetic reinforcement in transverse direction along embankment cross-section for full 3-d analysis.

ing the tension force in the longitudinal direction will be examined by comparing results to those obtained from a full 3-d analysis (with different degrees of nodal constraint specified along the bottom of the soft soil and GECs).

Figure 14 shows the variation of transverse tension force in the geosynthetic reinforcement along the embankment cross-section for a full 3-d analysis with "standard" and "increased" degrees of nodal constraint along the bottom boundary of the solution domain. The vertical grid lines in this figure coincide with the center of each GEC. The following observations can be made from Fig. 14:

1. The value of the reinforcement force in the full 3-d analysis with the standard degree of nodal constraint along the bottom boundary is noticeably greater (for this particular problem, by about 50%) than that obtained from a similar analysis with an increased degree of nodal constraint. This can be explained by the fact that some additional lateral resistance is provided in the case of increased degree of nodal constraint along the bottom boundary of the solution domain.
2. The maximum value of the reinforcement force in both analyses is almost constant from the embankment centerline up to the shoulder of the embankment (i.e., above the fifth GEC, which is located 6.4 m from the embankment centerline). After this point the force starts to decrease. This is because of larger embankment loads, combined with a greater tendency for lateral spreading of the reinforcement underneath the embankment from the centerline to the shoulder of the embankment, as compared to the reinforcement underneath the embankment slope.
3. In both analyses, the tension force above the center of each GEC has a minimum value, followed by two peaks at the edges of each column. It can also be observed that for the columns located between the embankment centerline up to the first GEC after the shoulder of embankment, the peak value at the right side of each column (i.e., toward the shoulder of the embankment) is always greater than that at the left side of the column (due to the lateral spreading to the right). This trend reverses for columns located beyond the first GEC on the right side of shoulder of the embankment. In this case, due to the embankment slope, higher loads are present at the left side of GECs than at the right.

Figure 15 shows the tension force in the geosynthetic reinforcement obtained from 3-d and axisymmetric unit cell idealizations, and the transverse tension force from a full 3-d analysis. From this figure, it is clear that the results of the 3-d and axisymmetric unit cell analyses are very close to each other. However, both analyses predict substantially lower tensile forces than those from the full 3-d analysis. In addition, for the unit cell analyses the maximum tensile forces occur above the center of the col-

umn and become zero over the soft soil at the mid span of columns. In the full 3-d analyses, the values of tension force start to increase from the center of the column, reaching their maximum value slightly before the edge of the column. The rather large difference between the tension forces in the transverse direction obtained from unit cell analyses and those obtained from a full 3-d analysis can be attributed to the lateral spreading of the embankment in the latter case.

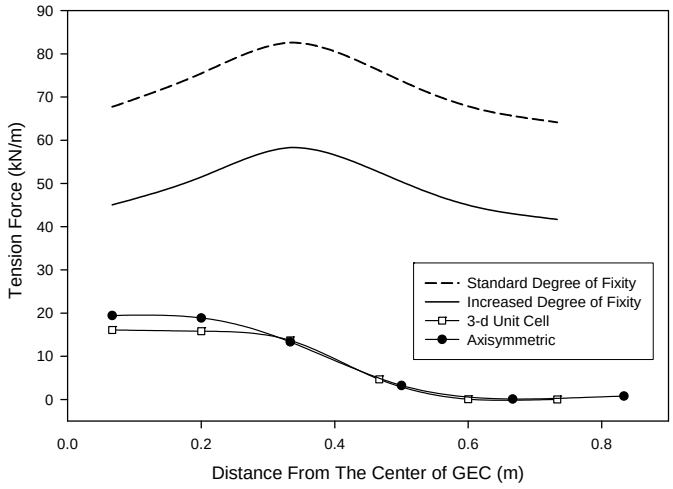

Fig. 15: Comparison of reinforcement force from full 3-d and unit cell analyses in the transverse direction.

Using Eq. (1) in conjunction with the friction angle and the unit weight of the embankment material (35° and 20 kN/m^3, respectively), and the height of the embankment (5 m), the tension force due to the lateral spreading is calculated to be 67.7 kN/m. This value is added to the tension forces obtained from unit cell analyses, and the results are shown in Fig. 16. For the sake of comparison, the results of a full 3-d analysis are also shown in this figure. It is clear that the corrected values of tensile forces from the unit cell analyses are in fairly good agreement with the results from the full 3-d analysis with the standard degree of nodal constraint along the bottom boundary of the solution domain. The corrected values of tensile forces from unit cell analyses, however, are overestimated when compared to the results from the full 3-d analysis with the increased degree of nodal constraint along the bottom boundary of the solution domain.

Figure 17 compares the reinforcement forces in the transverse and longitudinal directions obtained from a full 3-d analysis with an increased degree of nodal constraint along the bottom boundary. It is clear that the tension force in the transverse direction is always greater than that in the longitudinal direction. In particular, for the specific case considered herein, the maximum tension force in the transverse direction is 50% greater than the maximum value in the longitudinal direction. A similar trend was also found for model results when the standard degree of nodal constraint was applied along the bottom boundary.

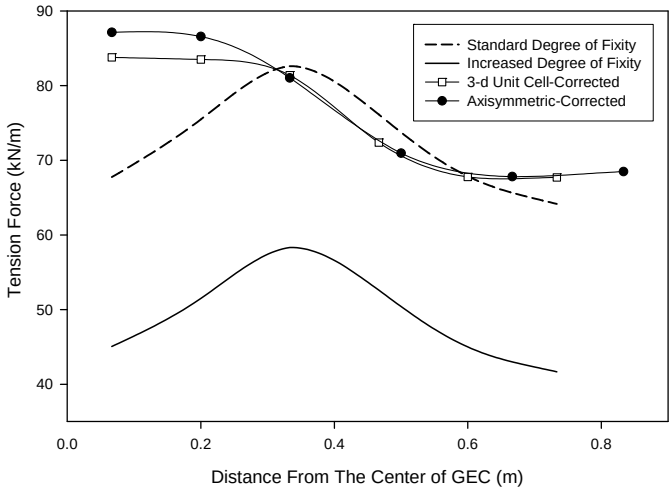

Fig. 16: Comparison of corrected reinforcement force from unit cell analyses and actual tension forces from full 3-d analyses in the transverse direction.

Figure 18 shows the tension force in the longitudinal direction obtained from a full 3-d analysis, together with that from the 3-d and axisymmetric unit cell analyses. From Fig. 18, a similar pattern of longitudinal tensile forces for the full 3-d analysis and for the 3-d and axisymmetric unit cell analyses is evident. This can be explained by the similarity of boundary conditions in the longitudinal direction for a full-3d model to those from the unit cell analyses. It is also clear from Fig. 18 that the longitudinal tensile forces from a full 3-d analysis are always greater than those predicted by the unit cell analyses. The maximum value of tensile force from the full 3-d analysis is about 3 times greater than the maximum values from the unit cell analyses. This is attributed to the fact that only in the full 3-d analysis is the transverse reinforcement force correctly computed. Since the geosynthetic acts like a membrane, it follows that the longitudinal force will likewise be affected in the full 3-d analysis.

As a result of these analyses, it can be reasonably concluded that the unit cell idealizations are not capable of properly predicting the values of the reinforcement forces in the longitudinal direction. These results (Fig. 18) disagree with the commonly accepted assumption that the longitudinal tension force in the geosynthetic reinforcement is equal to the tension force that is calculated from a unit cell idealization. Consequently, full 3-d analyses are required to more precisely compute the longitudinal forces in the geosynthetic reinforcement.

4 Conclusions

This paper has presented the results of finite element analyses of a hypothetical geosynthetic reinforced column supported embankment (GRCSE) with geosynthetic encased columns (GECs) as the deep foundation elements. The main focus of this study was the validity of the unit cell concept in the finite element modeling of GRCSEs with GECs. Full 3-d, 3-d unit cell, and axisymmetric unit cell

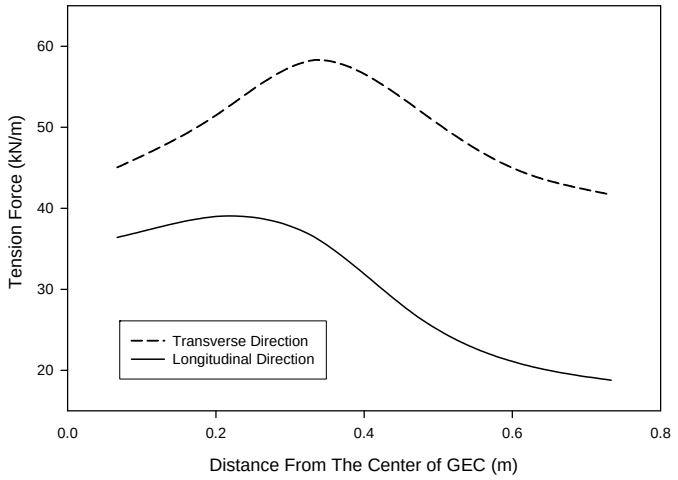

Fig. 17: Comparison of tension force in transverse and longitudinal directions from full 3-d analysis with increased degree of nodal constraint along the bottom boundary.

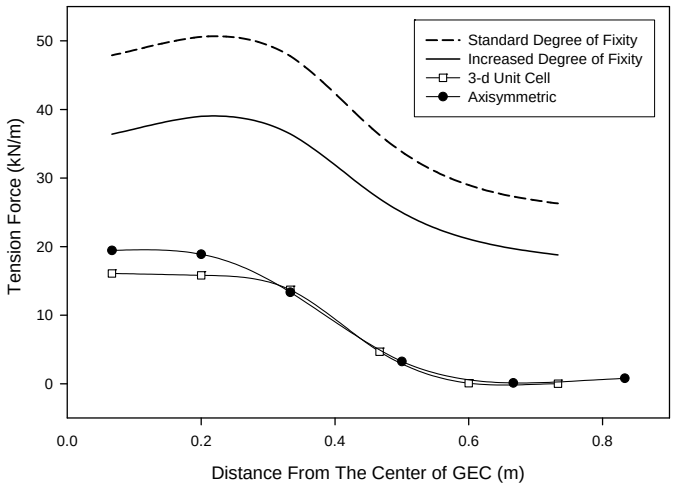

Fig. 18: Comparison of reinforcement force from unit cell and full 3-d analyses in the longitudinal direction.

analyses were carried out to simulate the response of a hypothetical GRCSE with GECs. Also investigated in this paper was the effect of the degree of nodal constraint along the bottom boundary of the solution domain when numerically modeling GRCSEs. The following conclusions were reached as a result of the finite element analyses that were performed:

1. Full 3-d analyses of the hypothetical 5 m high GRCSE analyzed herein showed that for embankment heights lower than 3 m, the results for columns located on the embankment centerline (i.e., the first column) and those directly under the shoulder of the embankment (i.e., at the fifth column) were insensitive to the distance of the column from the embankment centerline. As the height of embankment increased to 5 m, some differences were found between columns located on the embankment centerline and those directly under the shoulder of the embankment. The maximum difference between results from the first and fifth columns was found to be 12% for a full 3-d analysis with increased degree of nodal constraint along the bottom boundary of the solution domain, and 20% for a similar analysis with a standard degree of nodal constraint along the same boundary.
2. Axisymmetric unit cell analyses of the GRCSE yielded almost the same results as the 3-d unit cell analyses. A unit cell idealization, either 3-d or axisymmetric, can be used for numerical modeling of GRCSEs to successfully calculate a number of required design parameters such as: the average vertical stresses carried by the GECs, lateral displacement of the GECs and, to some extent, the maximum settlement of the soft foundation soil. Comparison of unit cell analyses with full 3-d analyses (with increased degree of nodal constraint along the bottom boundary) showed that, except for the tension force in the geosynthetic reinforcement, all parameters that were studied herein and calculated from unit cell analysis are in good agreement with those from a full 3-d analysis.
3. The results of finite element analyses proved that a full 3-d idealization is required to more precisely determine the tension forces produced in the geosynthetic reinforcement. It was found that the tension forces calculated from 3-d and axisymmetric unit cell analyses were significantly less than those calculated from a full 3-d analysis. This is explained by the fact that lateral spreading of the embankment and soft soil is accounted for in full 3-d analyses. Although the tension force in the geosynthetic may be estimated using a plane strain idealization, the accuracy of this estimate will decrease with increased inter-column spacing in the lateral direction.
4. Full 3-d analyses showed that tension forces in the transverse direction are greater than those in the longitudinal direction due to lateral spreading of the embankment. The maximum tension force in the transverse direction was found to be about 50% greater than the maximum value in the longitudinal direction.
5. The results of full 3-d analyses disagreed with the commonly accepted assumption that the longitudinal tension force in the geosynthetic reinforcement is equal to the tension force calculated from unit cell idealization. In particular, the maximum value of tension force in the longitudinal direction obtained from a full 3-d analysis was found to be about 3 times greater than the tension force calculated from unit cell analyses. Such differences are attributed to the fact that in the full 3-d analyses lateral displacement of the embankment and soft foundation soil is permitted, thus inducing higher transverse forces in the geosynthetic. Since the geosynthetic acts like a membrane, it follows that the tension force in the longitudinal direction would also be affected.
6. Finite element results showed that 3-d and axisymmetric unit cell analyses are generally unaffected by the nodal constraints imposed along the bottom

boundary of the GEC and the surrounding soft soil. This is explained by the fact that there is no lateral loading in the unit cell idealizations. For full 3-d analyses the results were, however, affected by the degree of nodal constraint in the transverse direction (x-direction) along the bottom boundary. This effect is attributed to the lateral spreading of the embankment. In particular, it was found that the results from the full 3-d analyses with a "standard" degree of nodal constraint along the bottom boundary differed from those calculated from similar analyses with an "increased" degree of nodal constraint along the bottom boundary. It was also found that the results of unit cell analyses were more similar to the results of a full 3-d analysis with an increased degree of nodal constraint along the bottom boundary. In reality, however, the bottom boundary is neither completely constrained in all directions nor it is free to move laterally. In other words, the behavior along the actual bottom boundary is likely somewhere between the two extremes of nodal constraint assumed in this study. In addition, the effect of the bottom boundary on the numerical results of a full 3-d analysis of GRCSEs is also expected to be dependent on the length of the deep foundation elements. In particular, as the length of these elements increases, the influence of the bottom boundary on the finite element results is expected to decrease. This effect, however, was not investigated as part of this study.

7. For the models with a "standard" degree of nodal constraint along the bottom boundary, the largest differences in results between the full 3-d and unit cell analyses were in the calculation of the settlement of the foundation soil and the maximum value of the lateral displacement of the GECs. This difference was typically found to be less than 20%. The difference in these results is expected to be even smaller if some fixity is present along the bottom boundary, which is a reasonable expectation for an actual GRCSE. Consequently, the authors feel that a unit cell idealization provides a reasonable approximation of the behavior that is obtained from full 3-d analyses for GRCSEs that are constructed using GECs. The only exception to this conclusion is the calculation of tensile forces that are induced in the geosynthetic reinforcement layer by the lateral spreading of the embankment in both the transverse and longitudinal directions.

Although the conclusions that are reached in this study cannot necessarily be generalized to all cases with different geometries and soil/geosynthetic properties, they do provide a useful indication of general trends in GRCSE behavior. Future experimental research is needed in this area to validate the simulation-based observations that are made herein.

Acknowledgments

This material is based upon work supported in part by the Geosynthetic Institute under its GSI Fellowship Program.

List of symbols

The following symbols are used in this paper:

c = Effective cohesion (Pa);
D = Column diameter (m);
D_e = Center-to-center column spacing (m);
e = Void ratio at unit pressure (dimensionless);
E = Effective Young's modulus (Pa);
J = Tensile modulus (N/m);
M = Slope of the critical state line (dimensionless);
ϕ = Friction angle (degree);
κ = The slope of the swelling line (dimensionless);
λ = The slope of the virgin consolidation line (dimensionless);
ν = Poisson's ratio (dimensionless);
ψ = Dilatancy angle (degree).

References

Alexiew D, Brokemper D, Lothspeich S (2005) Geotextile encased columns (GEC): load capacity, geotextile selection and pre-design graphs. In: Proceedings of the geofrontiers 2005 congress, Austin, Texas, pp 1-14

Al-Joulani N, Bauer GE (1995) Laboratory behavior of sleeve-reinforced stone columns. Geosynthetics '95 conference proceedings, pp 1111-1123

Almeida MSS, Hosseinpour I, Riccio M (2013) Performance of a geosynthetic-encased column (GEC) in soft ground: numerical and analytical studies. Geosynth Int 20(4):252-262

Balasubramanian AS, Chaudhry AR (1978) Deformation and strength characteristics of soft Bangkok clay. J Geotech Eng Div ASCE 104(9):1153-1167

Borges JL, Domingues TS, Cardoso AS (2009) Embankments on soft soil reinforced with stone columns: numerical analysis and proposal of a new design method. Geotech Geol Eng 27(6):667-679

Brooker EW, Ireland HO (1965) Earth pressures at rest related to stress history. Can Geotech J 2(1):1-15

BS 8006 (1995) Code of practice for strengthened/reinforced soils and other fills. BSI, Milton Keynes

Carlson BO (1987) Armerad Jord beräkningsprinciper för banker på pålar. Terranova, Distr. SGI., Linköping (in Swedish)

Castro J, Sagaseta C (2009) Consolidation around stone columns. Influence of column deformation. Int J Numer Anal Meth Geomech 33(7):851-877

Chen RP, Chen YM, Han J, Xu ZZ (2008) A theoretical solution for pile-supported embankments on soft soils under one-dimensional compression. Can Geotech J 45(5):611-623

Chew SH, Phoon HL, Hello BL, Villard P (2006) Geosynthetic reinforced piled embankment: large-scale model tests and numerical modeling. In: 8th International conference on geosynthetics, Geosynthetics, Yokohama, Japan, September 18-22, vol 1-4, pp 901-904

Collin JG (2004) Column supported embankment design considerations. In: Labuz JF, Bentler JG (eds) Proceedings of the 52nd annual geotechnical engineering conference, University of Minnesota, St. Paul, pp 51-78

Elias V, Welsh J, Warren J, Lukas R, Collin G, Berg RR (2006) Ground improvement methods, volume II, FHWA-NHI-06-020

Elsawy MBD (2013) Behaviour of soft ground improved by conventional and geogrid-encased stone columns, based on FEM study. Geosynth Int 20(4):276-285

Han J, Gabr MA (2002) Numerical analysis of geosynthetic-reinforced and pile-supported earth platforms over soft soil. J Geotech Geoenviron Eng 128(1):44-53

Han J, Wayne MH (2000) Pile-soil-geosynthetic interactions in geosynthetic reinforced platform/piled embankments over soft soil. In: Presentation at 79th annual transportation research board meeting, Washington, DC

Han J, Collin JG, Huang J (2004) Recent development of geosynthetic-reinforced column-supported embankments. In: Proceedings of the 55th highway geology symposium, Kansas City, Missouri, September 7-10, pp 299-321

Han J, Huang J, Porbaha A (2005) 2D numerical modeling of a constructed geosynthetic-reinforced embankment over deep mixed columns. ASCE Geotechnical Special Publication (GSP) No. 131: contemporary issues in foundation engineering, ASCE GeoFrontiers, Austin, TX, pp 24-26

Han J, Oztoprak S, Parsons RL, Huang J (2007) Numerical analysis of foundation columns to support widening of embankments. Comput Geotech 34(6):435-448

Hibbitt, Karlsson and Sorensen Inc. (2007) ABAQUS user's manual, version 6.7, Pawtucket, RI

Huang J, Han J, Collin JG (2006) Deformations of geosynthetic-reinforced column-supported embankments. In: Proceedings of the 8th international geosynthetics conference, 18-22 September, Yokohama, Japan, pp 1029-1032

Huang J, Han J, Oztoprak S (2009) Coupled mechanical and hydraulic modeling of geosynthetic-reinforced column-supported embankments. J Geotech Geoenviron Eng 135(8):1011-1021

Jenck O, Dias D, Kastner R (2009) Three-dimensional numerical modeling of a piled embankment. Int J Geomech 9(3):102-112

Jones CJPF, Lawson CR, Ayres DJ (1990) Geotextiles reinforced piled embankments. In: 4th international conference on geotextiles, geomembranes and related products, Den Haag, vol 1, pp 155-160

Kaliakin VN, Khabbazian M, Meehan CL (2012) Modeling the behavior of geosynthetic encased columns: influence of granular soil constitutive model. Int J Geomech ASCE 12(4):357-369. doi:10.1061/(ASCE)GM.1943-5622.0000084

Kempfert H-G, Gobel C, Alexiew D, Heitz C (2004) German recommendations for reinforced embankments on pile-similar elements. EuroGeo3: 3rd European geosynthetics conference, geotechnical engineering with geosynthetics, Munich, pp 279-284

Kempton G, Russell D, Pierpoint ND, Jones CJFP (1998) Two- and three-dimensional numerical analysis of the performance of piled embankments. In: Proceedings of the 6th international conference on geosynthetics, Atlanta, GA, pp 767-772

Khabbazian M (2011) Numerical simulation of geosynthetic encased columns used individually and in group configurations. A dissertation submitted to the Faculty of the University of Delaware in partial fulfillment of the requirements for the degree of Doctor of Philosophy in Civil Engineering

Khabbazian M, Kaliakin VN, Meehan CL (2009) 3D analyses of geosynthetic encased stone columns. In: Proceedings of international foundations congress and equipment expo 09 (IFCEE09), contemporary topics in ground modification, problem soils, and geo-support, geotechnical special publication No. 187, Orlando, FL, March 15-19, ASCE, pp 201-208

Khabbazian M, Kaliakin VN, Meehan CL (2010a) Numerical study of the effect of geosynthetic encasement on the behaviour of granular columns. Geosynth Int Thomas Telford 17(3):132-143

Khabbazian M, Meehan CL, Kaliakin VN (2010b) Numerical study of effect of encasement on stone column performance. In: Proceedings GeoFlorida 2010: advances in analysis, modeling & design, geotechnical special publication No. 199, West Palm Beach, FL, February 20-24, 2010, ASCE, Reston, VA, pp 184-193

Khabbazian M, Kaliakin VN, Meehan CL (2011a) Performance of quasilinear elastic constitutive models in simulation of geosynthetic encased columns. Comput Geotech 38(8):998-1007

Khabbazian M, Meehan CL, Kaliakin VN (2011b) Influence of granular soil constitutive model when simulating the behavior of geosynthetic encased columns. Geo-Frontiers 2011: advances in geotechnical engineering, geotechnical special publication No. 211, Dallas, TX, March 13-16, 2011, ASCE, Reston, VA, pp 539-548

Khabbazian M, Kaliakin VN, Meehan CL (2012) Numerical simulation of column supported embankments with geosynthetic encased columns: influence of soft soil constitutive model. Geo-Congress 2012: state of the art and practice in geotechnical engineering, geotechnical special publication no. 225, Oakland, CA, March 25-29, 2012, ASCE, Reston, VA, 1-10. doi:10.1061/9780784412121.001

Lawson CR (1992) Soil reinforcement with geosynthetics. Southeast Asian Geotechnical Society (SEAGS), Appl Ground Improv Tech, pp 55-74

Lee KL, Seed HB (1967) Drained strength characteristics of sands. J Soil Mech Found Div ASCE 93(6):117-141

Liu HL, Ng CWW, Fei K (2007) Performance of a geogrid-reinforced and pile supported highway embankment over soft clay: case study. J Geotech Geoenviron Eng 133(12):1483-1493

Lo SR, Zhang R, Mak J (2010) Geosynthetic-encased stone columns in soft clay: a numerical study. Geotext Geomembr 28(3):292-302

Malarvizhi SN, Ilamparuthi K (2007) Performance of stone column encased with geogrids. In: Proceedings of the 4th international conference on soft soil engineering, pp 309-314

McKelvey JA, III (1994) Consideration of equipment loadings in geosynthetic lined slope designs. In: Proceedings of the 8th international conference on computer methods and advances in geomechanics, Rotterdam, vol 2, pp 1371-1377

Murugesan S, Rajagopal K (2006) Geosynthetic-encased stone columns: numerical evaluation. Geotext Geomembr 24(6):349-358

Murugesan S, Rajagopal K (2007) Model tests on geosynthetic-encased stone columns. Geosynth Int 14(6):346-354

Oh YI, Shin EC (2007) Reinforcement and arching effect of geogrid-reinforced and pile-supported embankment on marine soft ground. Mar Georesour Geotechnol 25(2):97-118

Park S, Yoo C, Lee D (2007). A study on the geogrid reinforced stone column system for settlement reduction effect. In: Proceedings of the seventeenth international offshore and polar engineering conference, Lisbon, Portugal, July 1-6, pp 1636-1641

Plaut RH, Filz GM (2010) Analysis of geosynthetic reinforcement in pile-supported embankments. Part III: axisymmetric model. Geosynth Int 17(2):77-85

Pulko B, Majes B, Logar J (2011) Geosynthetic-encased stone columns: analytical calculation model. Geotext Geomembr 29(1):29-39

Russell D, Pierpoint N (1997) An assessment of design methods for piled embankments. Ground Eng 30(11):39-44

Smith M, Filz G (2007) Axisymmetric numerical modeling of a unit cell in geosynthetic-reinforced, column-supported embankments. Geosynth Int 14(1):13-22

Stewart ME, Filz GM (2005) Loads on geosynthetic reinforcement in bridging layers for pile-supported embankments. In: Proceedings of geo-frontiers 2005, ASCE, Austin

Tan SA, Tjahyono S, Oo KK (2008) Simplified plane-strain modeling of stone-column reinforced ground. J Geotech Geoenviron Eng 134(2):185-194

Vega-Meyer R, Shao Y (2005) Geogrid-reinforced and pile-supported roadway embankment. Geo-Frontiers 2005, contemporary issues in foundation engineering, geotechnical special publication no. 131, January 24-26, Austin, Texas

Wachman GS, Biolzi L, Labuz JF (2010) Structural behavior of a pile-supported embankment. J Geotech Geoenviron Eng 136(1):26-34

Yan L, Yang JS, Han J (2006) Parametric study of geosynthetic-reinforced pile-supported embankments. Advances in earth structures: research to practice, ASCE Geotechnical Special Publication No. 151. In: Yin J-H, White DJ, Han J, Lin G (eds) Proceedings of the GeoShanghai international conference 2006, Shanghai, China, June 6-8, pp 255-261

Yoo C (2010) Performance of geosynthetic-encased stone columns in embankment construction: numerical investigation. J Geotech Geoenviron Eng 138(8):1148-1160

Yoo C, Kim SB (2009) Numerical modeling of geosynthetic-encased stone column-reinforced ground. Geosynth Int 16(3):116-126

Zheng JJ, Chen BG, Lu YE, Abusharar SW, Yin JH (2009) The performance of an embankment on soft ground reinforced with geosynthetics and pile walls. Geosynth Int 16(3):173-182